

# Optical and chemical properties of vanadium oxide thin films prepared by vacuum arc discharge

O. MRAD<sup>a\*</sup>, I. M. ISMAIL<sup>a</sup>, B. ABDALLAH<sup>b</sup>, M. S. RIHAWY<sup>a</sup>

<sup>a</sup>Atomic Energy Commission, Department of Chemistry, P. O. Box 6091, Damascus, Syria

<sup>b</sup>Atomic Energy Commission, Department of Physics, P. O. Box 6091, Damascus, Syria

Vanadium oxide thin films have been prepared using vacuum arc discharge technique. Two sets of samples were prepared by altering two different experimental parameters, one by applying different chamber temperatures at constant gas mixture ratios ( $O_2 / Ar$ ) and the other by using different gas mixture ratios in the chamber at fixed temperature. The optical band gap of the films was evaluated using UV-vis-NIR scanning spectrophotometer, by recording transmittance spectra. X-ray photoelectron spectroscopy (XPS), was devised to obtain the chemical state of vanadium in the surface of the films. Elemental composition and thicknesses of the films have been estimated by means of Rutherford backscattering technique. A correlation between the optical properties of the films with the chemical structure was evaluated.

(Received November 06, 2013; accepted September 11, 2014)

**Keywords:** Gap energy, Vanadium oxides, Vacuum arc discharge, RBS, XPS

## 1. Introduction

Vanadium oxides ( $V_xO_y$ ) are widely used in many applications [1]. They can be applied as oxidation catalysts [2], in thermochromic window coating [3], in temperature and light sensors [4] and as cathodes in modern rechargeable batteries [5].

It is well known that vanadium displays multiple valence states (II to VII) in its compounds, including the oxides ( $V_xO_y$ ), which lead to both unique optical properties [6, 7] and changes in the electrical properties with metallic behavior in the case of  $x > y$  [8], and semiconductor properties in the case of  $x < y$  [9].

Vanadium oxide thin films can be successfully prepared by a large variety of deposition techniques [10], such as pulsed laser deposition (PLD), inverted cylindrical magnetron sputtering (ICMS) [11], r. f. and d. c. reactive sputtering [12, 13] and sol-gel technique [14].

In this work, we aim to prepare vanadium oxide thin films by vacuum arc discharge technique that could be operated at industrial level. Despite the low cost and large production capability of this technique, it has not been widely used for the preparation of vanadium oxide films, as far as we know. In order to produce  $V_xO_y$  films, two sets of samples were prepared, one at different chamber temperatures and the other using varying oxygen fraction in oxygen-argon gas mixtures.

Also, optical properties of the films were determined by the direct band gap energy ( $E_g$ ) measurement using UV-vis-NIR scanning spectrophotometer. The interpretation of the results of optical properties of the films was investigated by characterization of the films using both XPS and RBS techniques. X-ray photoelectron spectrometry (XPS) is used to access the chemical states of the surfaces. Rutherford Backscattering technique

(RBS) is employed to reveal information about the films thicknesses and atomic stoichiometry.

## 2. Materials and methods

$V_xO_y$  thin films were prepared by vacuum arc deposition using an industrial V-1000 "U" system from a pure vanadium target (99.9%). The vanadium target was first cleaned by pure argon discharge for 10 minutes prior to thin film deposition. Then, the films were deposited, on pure carbon substrates for RBS measurements in order to obtain a clear oxygen RBS signal separated from the substrate signal and also on glass substrates for optical studies using UV analysis. We have assumed that no differences in film composition or thickness may occur in relationship to substrate type; since our attention was paid to the influences of deposition conditions on the properties of the  $V_xO_y$  thin films rather than the substrate selection. This approach was discussed by some researchers such as Taabouche et al 2013 [15]. The XPS measurements were performed on films deposited on both kinds of substrates and gave similar results as expected since XPS probes the first thin layer (about 10 nm). The deposition time was set at 15 min for all samples to obtain films of about 300 nm thick. The residual pressure in the chamber was lower than  $3 \cdot 10^{-6}$  Torr and the working pressure was about  $2 \cdot 10^{-3}$  Torr. The substrates were rotated continuously around the vertical central axis of the vacuum chamber at a speed of 1.5 rpm. The arc current was maintained at 100 A during deposition. The films were prepared at two different conditions, either at varying chamber temperatures or using variable gas mixture ( $O_2/Ar$ ) ratios, while other experimental parameters (pressure, time,...etc.) were kept unchanged. The first group was prepared at a fixed oxygen-argon gas mixture (25%  $O_2$ , 75% Ar), while the chamber was operated at temperatures of 50 °C, 100°C,

200 °C and 300 °C. The second series was prepared at a chamber temperature of 50 °C, while the Ar-O<sub>2</sub> gas mixture was varied (i.e. oxygen gas contents were 15%, 25%, 50%, 75% or 100%).

The optical properties were determined using UV-vis-NIR scanning spectrophotometer, (Shimadzu UV-3101 PC) by recording transmittance spectra.

The chemical composition of the films has been measured by X-ray photoelectron technique. The XPS analyses were performed using the SPECS UHV/XPS/AES system with a hemispherical energy analyzer. The monochromated Al K<sub>α</sub> X-ray (1486.6 eV) is used as the excitation source and is operated at 250 W. The cleaning of the film surface contamination during time between preparation and analysis is processed by bombardment of 5 keV argon ion beam. In all films, carbon peak (C 1s about 285 eV) has disappeared after cleaning. High resolution spectra of the O 1s and V 2p peaks are treated and deconvoluted with CasaXPS software (version 2.3.16Dev52) using a non-linear least-squares method with a Gaussian/ Lorentzian peak shape GL(30) and the background was subtracted using the Shirley method [16, 17].

The RBS measurements were performed on the V<sub>x</sub>O<sub>y</sub> thin films deposited on carbon substrates. It is utilized to both obtain O/V atomic ratio and verify the thicknesses of the films. <sup>4</sup>He<sup>2+</sup> ion beam of energy of 2 MeV was produced using 3 MV HVEE™ tandem accelerator [18] at the Atomic Energy Commission of Syria (AECS). Backscattered alpha particles were detected using Canberra's passivated ion-implanted (PIPS) detector (Model No. PD50-12-100AM) with resolution of 12 keV and active area of 50 mm<sup>2</sup>. It is placed at 165° with respect to the beam and at a distance of 4 cm from the sample. The beam spot size was set to 2 × 2 mm<sup>2</sup> using two set of beam collimators placed in the beam line. The data were recorded on a PC MCA using MCDWIN software v.2.87 from FAST ComTec. The RBS spectra were treated using the computer simulation code SIMNRA [19].

### 3. Results and discussion

#### 3.1 Part I: Films prepared at varying chamber temperatures

##### 3.1.1 Optical properties

The direct band gap energy ( $E_g$ ) for the sample is determined by fitting the absorption data to the direct transition equation:

$$\alpha hv = B (hv - E_g)^{1/2}$$

where  $\alpha$  is the optical absorption coefficient at photon energy,  $hv$  is the photon energy, and  $B$  is a constant [20]. As an example, the UV-visible transmission spectrum of the sample prepared at 200 °C is shown in Fig 1.  $E_g$  is obtained by plotting  $(\alpha hv)^2$  as a function of  $hv$ , and subsequently extrapolating the linear portion of the curve to the absorption equal to zero as shown in Fig. 2. For instance, the optical band gap ( $E_g$ ) is evaluated as 3.06 eV for the selected case.

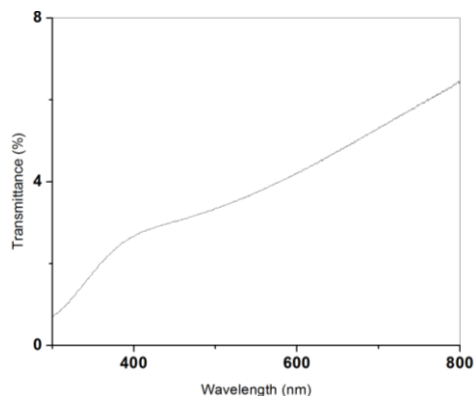


Fig. 1. Transmittance of the sample prepared at chamber temperature of 200 °C.

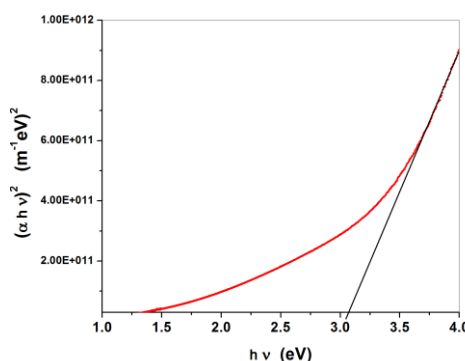


Fig. 2. plot of  $(\alpha hv)^2$  as a function of photon energy ( $hv$ ) of the sample prepared at chamber temperature 200 °C.

Fig. 3 gives the values of the band gap ( $E_g$ ) for the prepared samples as a function of chamber temperatures. It can be noticed that  $E_g$  tends to increase with the temperature. The values lies in the range between 2.88 to 3.35 eV. This trend can be explained by the variation of the vanadium oxidation state. It has been demonstrated that higher oxidation state of vanadium is associated with smaller  $E_g$ , and vice versa [21]. In order to investigate whether such effect is taking place or not in our case, the oxidation states of vanadium will be determined by XPS measurements.

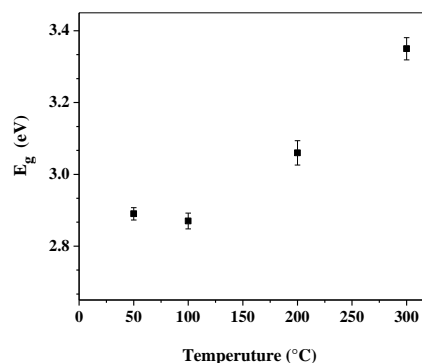


Fig. 3.  $E_g$  values as a function of the chamber temperature for the samples prepared at different chamber temperatures.

### 3.1.2 XPS measurement

Fig. 4 presents typical high resolution spectra of O 1s and V 2p for the sample prepared with 25% O<sub>2</sub> (75% Ar) at 50 °C. Principal peaks corresponding to oxygen (O 1s) and vanadium (V 2p<sub>1/2</sub> and V 2p<sub>3/2</sub>) were inspected at 530 eV, 524 eV and 516 eV, respectively [22, 23].

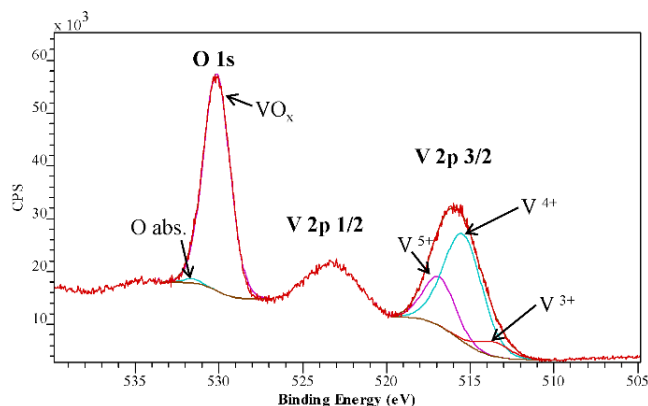


Fig. 4. XPS high resolution spectra for sample prepared with 25% O<sub>2</sub> at 50 °C.

The deconvolution of O 1s spectrum gives two components, that correspond to V-O at about 530 eV binding energy (BE) and small peak at higher binding energy which can be attributed to the adsorbed oxygen or OH (BE= 531.4 eV) [23]. The overlapping of the oxygen peaks that are resulting from V<sub>2</sub>O<sub>3</sub> (530.0 eV), VO<sub>2</sub> (530.0 eV) and V<sub>2</sub>O<sub>5</sub> (529.8 eV) [23-25] have made the individual peaks difficult to discern them from the other. Thus, it was not possible to determine the oxidation state of vanadium from the oxygen peak (O 1s). Therefore, the V 2p<sub>3/2</sub> spectrum was only considered. V 2p<sub>3/2</sub> can be assigned to V<sup>3+</sup> (BE= 515.3 eV), V<sup>4+</sup> (BE= 516.3 eV), and V<sup>5+</sup> (BE= 517.5 eV) [26, 27]. The competition of these states was investigated as a function of the preparation conditions. In resume, the V<sub>x</sub>O<sub>y</sub> film prepared at 50 °C is composed of mixture of V<sub>2</sub>O<sub>3</sub> (8%), VO<sub>2</sub> (67%) and V<sub>2</sub>O<sub>5</sub> (25%) chemical states. Therefore, the total O/V ratio on the surface was found to be 2.

Table 1 shows the evolution of V 2p<sub>3/2</sub> components of films prepared at different chamber temperature together with the O/V ratios on the surface. As the temperature of preparation increases, the V<sup>5+</sup> component decreases from 25 to 4 %. While V<sup>3+</sup> and V<sup>4+</sup> components concentration increases from 8 % and 67 % to 19 % and 77 %, respectively. Also it shows that no changes to the O/V ratios occurred on the surface of the films prepared at different chamber temperatures.

Table 1. the contribution of V 2p<sub>3/2</sub> components and O/V ratios for films prepared at different chamber temperatures (at constant gas mixture).

Temperature (°C)	V <sup>3+</sup> (%)	V <sup>4+</sup> (%)	V <sup>5+</sup> (%)	O/V
50	7.9	67.0	25.1	2.1
100	8.1	67.0	24.9	2.1
200	14.2	69.9	15.8	2.0
300	18.6	77.1	4.3	1.9

### 3.1.3 RBS measurement

Fig. 5 shows RBS spectrum for the sample prepared at 50 °C (25 % O<sub>2</sub>) together with the fit obtained from SIMNRA software [19]. The experimental data on the elastic scattering cross-section of alpha particles on light elements are integral to this software and can be used effectively for quantitative analysis of light elements; where the backscattered alpha particles might behave non-Rutherford backscattering. Both vanadium and oxygen peaks on the spectra are well separated from the carbon substrate signal. Therefore, the elemental composition and the thicknesses were easily processed and extracted. From the fit, the atomic percent (at. %) of both oxygen and vanadium is found to be 60 and 40 % respectively, which gives average O/V atomic ratio of 1.5 in the whole thickness of the film. We can notice a slight rise near the oxygen peak edge which corresponds to higher content of oxygen at the surface of the film due to the further exposure to the oxygen in the chamber. This finding is consistent with the XPS results at the surface (O/V ratio is 2). The film thickness is also evaluated from the RBS spectrum (about 1750×10<sup>15</sup>at/cm<sup>2</sup>). Excluding the near surface, the obtained elemental profiles show uniform distribution of both vanadium and oxygen on the carbon substrate, which suggests good deposition of the film.

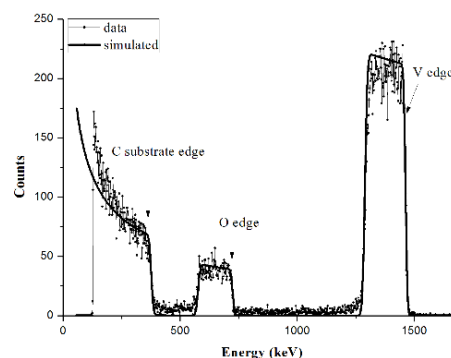


Fig. 5. RBS spectrum of for the sample prepared at 50 °C (25 % O<sub>2</sub>).

The same treatment was applied to the other films and the atomic stoichiometry was then deduced and summarized in table 2. It is clear that the alteration of the temperature during sample preparation gives no significant changes in both O/V atomic ratios and the film thicknesses. However the chamber temperature plays a role in the oxidation states of vanadium as seen by XPS.

Table 2. Atomic ratios of V and O together with the film thicknesses obtained from RBS data for films prepared at different chamber temperatures (25 % O<sub>2</sub>).

T (°C)	V (at. %)	O (at. %)	O/V	Thickness (10 <sup>15</sup> at./cm <sup>2</sup> )
50	40.4	59.6	1.5	1750
100	41.5	58.5	1.4	1788
200	38.3	61.7	1.6	1725
300	38.5	61.5	1.6	1707

### 3.2 Part II: Films prepared at varying oxygen ratios

#### 3.2.1 Optical properties

The band gap energy values for the samples prepared at different oxygen gas ratios (at fixed chamber temperature of 50 °C) were calculated and illustrated in Fig. 6. Generally, the band gap energy values decrease with the increase of the oxygen ratios. As previously mentioned, this phenomenon is occurred due to the increase in the oxidation state of vanadium. These result will be confirmed by XPS measurements.

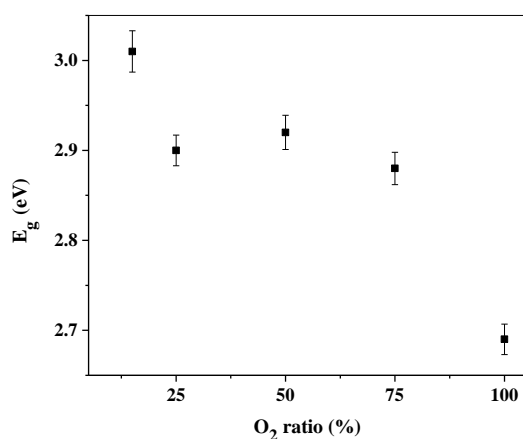


Fig. 6. E<sub>g</sub> values as a function of the oxygen gas ratios for the samples prepared using varying oxygen fraction in the O<sub>2</sub>/Ar gas mixtures.

#### 3.2.2 XPS measurement

The V 2p<sub>3/2</sub> high resolution spectra for the samples (prepared at different oxygen gas ratios) were deconvoluted into three components correspond to three oxidation states of vanadium. Table 3 summarizes the contribution of these oxides according to oxygen gas ratios

(at constant chamber temperature of 50 °C) together with the O/V ratios on the surface. The V<sup>3+</sup> and V<sup>4+</sup> components contributions decrease from 9 % and 71 % to 0 % and 56 %, respectively. While the V<sup>5+</sup> component increases from 20 to 44 %. This means that the increase in the oxygen gas ratios during preparation is accompanied with an increase in the oxidation state of vanadium. The table 3 shows that no changes happened to the O/V ratios on the surface of the films prepared at different oxygen gas ratios.

Table 3. The contribution of V 2p<sub>3/2</sub> components for different oxygen gas ratios films (at constant temperature 50 °C).

O <sub>2</sub> gas ratios (%)	V <sup>3+</sup> (%)	V <sup>4+</sup> (%)	V <sup>5+</sup> (%)	O/V
15	8.9	71.1	20.0	2.1
25	7.6	67.2	25.1	2.1
50	7.6	61.6	30.8	2.1
75	1.5	57.2	41.3	2.2
100	0.1	55.8	44.1	2.2

#### 3.2.3 RBS measurement

The atomic percent of both oxygen and vanadium in the films and their thicknesses were verified by means of RBS and illustrated in Table 4. It shows that the increase in the oxygen gas mixture during sample preparation is associated with an increase in the average O/V atomic ratios with no major change in the film thicknesses. It is obvious that the increase of O/V atomic ratios in the film bulk can be ascribed to the increase of oxygen gas ratio in the chamber during film deposition. It is clear from Table 4 that when the oxygen content is more than 50%, the average O/V ratios in the bulk (measured by RBS) tend to 2.5. This means that film prepared at higher oxygen gas ratio in the chamber is likely to form vanadium oxide with higher oxidation states.

Table 4. Atomic ratios of V and O together with the film thicknesses obtained from RBS data for films prepared at different oxygen gas ratios (at 50 °C).

O <sub>2</sub> gas ratios (%)	V (at. %)	O (at. %)	O/V	Thickness (10 <sup>15</sup> at./cm <sup>2</sup> )
15	41.3	58.7	1.4	1805
25	40.4	59.6	1.5	1750
50	32.5	67.5	2.1	1704
75	30.1	69.9	2.3	1715
100	29.3	70.7	2.4	1896

#### 4. Conclusions

$V_xO_y$  films were prepared by vacuum arc discharge technique. Two sets of samples were prepared with two different experimental conditions. The first set was prepared at different chamber temperatures while the second set was made by varying the chamber gas mixture  $O_2/Ar$  ratio. The chamber temperature and oxygen gas ratios play a major role in the transmittance of the films, where the vanadium oxide thin films were obtained with different band gap energies due to the change in the sample preparation procedure. It is concluded that the band gap energy values for the samples increase with the chamber temperatures and decrease with the oxygen gas ratio in the chamber. This behavior was attributed to the variation of the oxidation state of the vanadium in the films as shown by means of careful analysis of XPS measurements. They showed that higher oxidation states of vanadium were accompanied with lower values of  $E_g$ . RBS measurements show uniform distribution of vanadium in the deposited films with same thicknesses.

The O/V ratios obtained from both XPS and RBS measurements have shown apparent discrepancy where XPS results have higher values of O/V ratios compared to those obtained by RBS. This behavior can be attributed considering the fundamentals of both techniques (i.e. XPS technique can monitor the top surface layer while RBS can probe deeper thickness of the sample). The higher values of the O/V ratios obtained by XPS results correspond to higher content of oxygen at the surface of the film due to the further exposure to the oxygen in the chamber.

This study has demonstrated the feasibility of vanadium oxide thin films deposition by an industrial low cost technique, namely vacuum arc discharge.

#### Acknowledgements

The authors like to thank Prof. Dr. I. Othman the Director General of the Atomic Energy Commission of Syria and Prof. Dr. T. Yassin (head of chemistry department) for their encouragement.

#### References

- [1] Gail R. Willsky, Esther S. Takeuchi, Alan S. Tracey. (Taylor & Francis Group, New York, 2007).
- [2] Alette G. J. Ligtenbarg, Ronald Hage, Ben L. Feringa, *Coord. Chem. Rev.* **237**(1-2), 89 (2003).
- [3] P. Jin, G. Xu, M. Tazawa, K. Yoshimura, *Appl. Phys. A Mater. Sci. Process.* **77**, 455 (2003).
- [4] David O. Scanlon, Aron Walsh, Benjamin J. Morgan, Graeme W. Watson, *J. Phys. Chem. C* **112**, 9903 (2008).
- [5] Arturo Talledo Hector Valdivia, *J. Vac. Sci. Technol. A* **21**(4), 1494 (2003).
- [6] Wei-Tao Liu, J. Cao, W. Fan, Zhao Hao, Michael C. Martin, Y. R. Shen, J. Wu, F. Wang, *Nano Lett.* **11**(2), 466 (2010).
- [7] Jacques Livage, *Coord. Chem. Rev.* **190–192**(0), 391 (1999).
- [8] F. J. Morin, *Bell System Technical Journal* **37**(4), 1047 (1958).
- [9] Sakae Takeuchi, Kenji Suzuki, *J. Japan Inst. Metals* **33**(4), 409 (1969).
- [10] J. M. McGraw, J. D. Perkins, J. G. Zhang, P. Liu, P. A. Parilla, J. Turner, D. L. Schulz, C. J. Curtis, D. S. Ginley, *Solid State Ionics* **113–115**, 407 (1998).
- [11] Jeanne M. McGraw, Christian S. Bahn, Philip A. Parilla, John D. Perkins, Dennis W. Readey, David S. Ginley, *Electrochim. Acta* **45**, 187 (1999).
- [12] Anna Maria Salvi, Maria Rachele Guascito, Angela DeBonis, Francesca Simone, Agostino Pennisi, Franco Decker, *Surf. Interface Anal.* **35**, 897 (2003).
- [13] E. Kusano, J. A. Thell, J. A. Thornton, *J. Vac. Sci. Technol.* **A6**, 1663 (1988).
- [14] D. Alamarguy, J. E. Castle, N. Ibris, A. M. Salvi, *Surf. Interface Anal.* **38**, 801 (2006).
- [15] A. Taabouche, A. Bouabellou, F. Kermiche, F. Hanini, S. Menakh, Y. Bouachiba, T. Kerdja, C. Benazzouz, M. Bouafia, S. Amara, *Adv. Mater. Phys. Chem.* **3**, 209 (2013).
- [16] Neal Fairely, (Casa Software Ltd, 2009).
- [17] D. A. Shirley, *Physical review B* **5**, 4709 (1972).
- [18] D. J. W. Mous, A. Gottdang, R. van den Broek, R.G. Haitsma, *Nucl. Instr. and Meth. B* **99**, 697 (1995).
- [19] M. Mayer. (Max-Planck-Inst. Plasmaphy: Garching, Germany, 1997).
- [20] E. Ziegler, A. Heinrich, H. Oppermann, G. Stöver, *Phys. Status Solidi A* **66**(2), 635 (1981).
- [21] S. Tanemura, L. Miao, Y. Kajino, Y. Itano, M. Tanemura, S. Toh, K. Kaneko, Y. Mori, *J. Mater. Sci.: Mater. Electron.* **18**, S43 (2007).
- [22] John F. Moulder, William F. Stickle, Peter E. Sobol, Kenneth D. Bomben. (Physical Electronics Division, Perkin-Elmer Corporation, 1992).
- [23] Geert Silversmit, Diederik Depla, Hilde Poelman, Guy B. Marin, and Roger De Gryse, *J. Electron. Spectrosc. Relat. Phenom.* **135**(2-3), 167 (2004).
- [24] J. Mendialdua, R. Casanova, Y. Barbaux, *J. Electron. Spectrosc. Relat. Phenom.* **71**(3), 249 (1995).
- [25] E. Hryha, E. Rutqvist, L. Nyborg, *Surf. Interface Anal.* **44**(8), 1022 (2012).
- [26] Arturo Talledo Hector Valdivia, *J. Vac. Sci. Technol. A* **21**(4), 1494 (2003).
- [27] Y. Suchorski, L. Rihko-Struckmann, F. Klose, Y. Ye, M. Alandjiyska, K. Sundmacher, H. Weiss, *Appl. Surf. Sci.* **249**, 231 (2005).

\*Corresponding author: cscientific@aec.org.sy